Atmos. Chem. Phys. Discuss., https://doi.org/10.5194/acp-2019-60
Manuscript under review for journal Atmos. Chem. Phys.
Discussion started: 13 March 2019

Atmospheric Chemistry and Physics Discussions

Variation of size-segregated particle number concentrations in winter Beijing

Ying Zhou[1], Lubna Dada[1,2*], Yiliang Liu[3], Yueyun Fu[4], Juha Kangasluoma[1,2], Tommy Chan[1], Chao Yan[2], Biwu Chu[2], Kaspar R Daellenbach[2], Federico Bianchi[2], Tom Kokkonen[2], Yongchun Liu[1], Joni Kujansuu[1,2], Veli-Matti Kerminen[2], Tuukka Petäjä[2], Lin Wang[3], Jingkun Jiang[4], Markku Kulmala[1,2*]

[1]Aerosol and Haze Laboratory, Beijing Advanced Innovation Center for Soft Matter Science and Engineering, Beijing University of Chemical Technology, Beijing, China

[2]Institute for Atmospheric and Earth System Research / Physics, Faculty of Science, University of Helsinki, Finland

[3]Shanghai Key Laboratory of Atmospheric Particle Pollution and Prevention (LAP[3]), Department of Environmental Science & Engineering, Jingwan Campus, Fudan University, Shanghai 200438, China

[4]School of Environment, Tsinghua University, Beijing, China

*Correspondences are to Lubna Dada: lubna.dada@helsinki.fi and Markku Kulmala: markku.kulmala@helsinki.fi

Abstract

Aerosol number concentration varying spatially and temporally is a good indicator of the dynamic behavior of Beijing's atmospheric cocktail. This variation represents the strength of different contributing primary and secondary sources such as traffic and new particle formation, respectively. In this paper we report size-segregated particle number concentrations observed at newly developed Beijing station during winter 2018. Our measurements cover number size distributions of particles in a diameter range between 1.5 nm and 1 μm (cluster mode, nucleation mode, Aitken mode and accumulation mode), thus being descriptive of a major fraction of the processes happening in the atmosphere of Beijing. Here we aim to explain the concentration variation in the observed modes by relating them to potential aerosol sources as well as to understand the connection between the modes. We focused on two types of days (haze and new particle formation) and divided the data accordingly. Our results show that during new particle formation (NPF) days, an increase in the cluster mode particles was observed. In contrast, during haze days we observed a high concentration of accumulation mode particles. There was a clear correlation between the cluster and nucleation modes during NPF days, while it was absent during haze days. In addition, we correlated the different modes with concentrations of trace gases and other parameters measured at our station. Our results show that all modes in the sub-micron size range correlated with NO_x which

Atmos. Chem. Phys. Discuss., https://doi.org/10.5194/acp-2019-60
Manuscript under review for journal Atmos. Chem. Phys.
Discussion started: 13 March 2019

Atmospheric Chemistry and Physics Discussions

clearly reflects the contribution of traffic to all particle sizes.

1 Introduction

Atmospheric aerosols are the main ingredient of China's pollution cocktail (Kulmala 2015). They have gained increasing attention due to their effects on human heath, climate and visibility (Lelieveld et al., 2015, IPCC 2007). Currently, air quality standards for cities in China consider particle mass instead of number concentration (WHO, 2000), which may ignore the effect of ultra-fine particles (diameter less than 100 nm). However, it has been shown that ultra-fine particles can penetrate deep into the respiratory tract ending up to the blood circulation which allow them to deposit into the brain (Oberdörster et al., 2004). Indeed, studies have pointed out that ultra-fine particles, which contribute to a negligible fraction of the mass concentration, dominate the total number concentration in urban areas (von Bismarck-Osten et al., 2013;Wehner et al., 2004;Wu et al., 2008). Due to their high concentration, ultrafine particles' toxicological effect is enlarged by their large total surface area (Kreyling et al., 2004).

Apart from their health effects, the temporal and spatial variation of particle number concentrations of different sizes is a good estimate of the strength of their emission sources. The aerosols are emitted either directly as primary particles, such as sea salt or dust particles as a result of natural phenomena (Solomos et al., 2011), or nano-particles could also form through new particle formation (Kulmala, 2003; Kulmala et al., 2004; Kulmala et al., 2013; Kerminen et al., 2018; Chu et al., 2019). The newly formed particles can grow up into 20-100 nm within a day (Kulmala et al., 2004) and are found to contribute to a major fraction of cloud condensation nuclei (CCN), thus indirectly affecting the climate (Kerminen et al., 2012). For all aforementioned reasons and in order to form a collective, complete picture about atmospheric particles, to understand their origin and potential impacts at a specific location, the whole size distribution of these atmospheric particles needs to be studied.

Recently, due to urbanization and increased population, megacities have increased their contribution to atmospheric aerosol pollution massively (Baklanov et al., 2016). Interestingly, more people live in eastern Asia (specifically, China and India) rather outside (https://www.unfpa.org/swop). Therefore, it is important to study the contributions of different sources to size-segregated number concentrations in order to inspire policy makers and the public on measures that need to be taken in order to reduce particulate pollution. Many studies in various cities in China have tackled this topic. For instance, a two-years observation of particle number size distributions at a site northern Beijing reported that traffic emissions are the major source of nucleation (3-20 nm) and Aitken (20-100 nm) mode particles in urban Beijing (Wang et al., 2013). On another hand, a research conducted in western downtown of Nanjing reported that

local new particle formation events are the main contributors of nucleation (5-20 nm) mode and CCN (Dai et al., 2017). Moreover, an observation of nucleation mode particle concentration in urban Hong Kong reported the dominant contribution of combustion sources to nucleation mode (5.5-10 nm) (Wang et al., 2014a). Also, an observation in urban Guangzhou found that accumulation and secondary transformation of particles are the main reasons for high concentration of accumulation mode particles (100-660 nm) (Yue et al., 2010). However, only a few studies in China have reported measurements of cluster mode particles (sub-3 nm) and related them to new particle formation events (Cai et al., 2017;Xiao et al., 2015;Yao et al., 2018;Yu et al., 2016).

The observation of sub 3 nm particles and ions was made possible by recent major instrumentation development such as particle size magnifier (PSM) (Vanhanen et al., 2011), diethylene glycol-based scanning mobility particle sizer (DEG-SMPS) (Jiang et al., 2011), and Neutral Cluster and Air Ion Spectrometers (NAIS) (Manninen et al., 2016;Mirme et al., 2007).

In a complicated environment such as in Beijing, it is very hard to relate each particle mode to a specific source. Indeed, many sources could contribute to particles in the same size range. For instance, cluster mode particles mainly originate from the secondary gas-to-particle transformation process (Kulmala et al. 2013), although recently also traffic has been identified as a source for these small sized particles (Rönkkö et al., 2017). While these particles can grow to nucleation mode sizes, other sources such as black carbon from traffic contribute to Aitken mode, complicating the story even further (Pirjola et al., 2012). Various anthropogenic activities and biogenic processes contribute to accumulation mode sizes. Thus, correlating trace gases and aerosol concentrations of different sizes during different time periods help narrow down these aerosol sources.

In this study, we analyzed the number concentration of four sub-micron aerosol modes: cluster mode (sub-3 nm), nucleation mode (3-25 nm), Aitken mode (25-100 nm), and accumulation mode (100-1000 nm). Our aims are i) to investigate the number concentration variations of the size segregated aerosol number concentrations for each modes, ii) to explore the relationships between the modes under different atmospheric conditions, iii) to connect the number size distribution modes with multiple trace gases (NO_x, SO_2, CO and O_3) and $PM_{2.5}$ (particulate matter with aerodynamic diameter less than 2.5 μm), and iv) to quantify the contribution of NPF and haze formation to different particle modes in winter time in Beijing. Our work increases our understanding of the sources of the different sized particles in Beijing, China, and the work complements studies in other megacities.

Atmos. Chem. Phys. Discuss., https://doi.org/10.5194/acp-2019-60
Manuscript under review for journal Atmos. Chem. Phys.
Discussion started: 13 March 2019

2 Materials and Methods

2.1 2.1 Description of SMEAR Beijing station

Beijing, as the capital of China, accommodates more than 20 million people within 16.8 thousand square kilometers and only 1.4 thousand square kilometers for urban areas, with an expanding economic activity, construction and industry. Beijing, as one of the largest megacities in the world, is located in the Northern Chinese Plain, and is one of most industrialized regions in China. Mountains surround Beijing from the west, north and north-west.

For our study, we analyzed data collected at the newly developed station which is part of the Aerosol and Haze Laboratory in Beijing. The urban station follows from the concept of Station for Measuring Ecosystem and Atmospheric Relations (SMEAR) (Hari and Kulmala, 2005). Our station is located on the western campus of Beijing University of Chemical Technology (BUCT). It is constructed on the fifth floor of the teaching building on the campus and the sampling lines extend to the rooftop of the building around 20 m above the ground level. The station represents a typical area in urban Beijing subject to pollution sources, such as traffic, cooking and long-range transport of pollution. The campus is surrounded by highways and main roads from the East (3rd ring main road), north (Zizhu road) and south east (Zizhu Bridge). From the east, west and south, the campus is surrounded by residential and commercial areas.

Measurements at SMEAR Beijing started on 16 January, 2018 and continue until present except during the necessary instruments' maintenance and unavoidable factors such as power cuts (Lu et al., 2018). The data included in this study were collected between 16 January and 15 March 2018, representative of Beijing winter conditions.

2.2 Instrumentation

For a comprehensive measurement of particles, a full set of particle measuring instrumentation was operated. First, a nano-condensation nucleus counter system (nCNC) consisting of a Particle Sizer Magnifier (PSM, model A10, Airmodus Oy, Finland) and butanol condensation particle counter (CPC) (model A20, Airmodus Oy, Finland) measured number concentration of small clusters / particles of 1.2-2.5 nm (mobility diameter) (Vanhanen et al., 2011). To minimize the sampling losses, the PSM was sampling horizontally from window to the north through a short stainless steel sampling inlet extending ~1.2 m outward from the building. The length of the sampling tube was 1.33 m and the inner diameter is 0.8 cm. To further improve the sampling efficiency, a core sampling tube (Kangasluoma et al., 2016) was utilized. The total flow

Atmos. Chem. Phys. Discuss., https://doi.org/10.5194/acp-2019-60
Manuscript under review for journal Atmos. Chem. Phys.
Discussion started: 13 March 2019

rate was 7.5 liters per minute (lpm), from which 5 lpm was used as a transport flow while the nCNC sample flow rate was 2.5 lpm. In the operation of the PSM the saturator flow scanned from 0.1 to 1.3 lpm within 240s.

A particle size distribution (PSD) system measured aerosol size distribution of 3 nm-10000 nm (Liu et al., 2016). It included a nano-scanning mobility particle sizer (nano SMPS, 3-55 nm, mobility diameter), a long SMPS (25-650 nm, mobility diameter) and an aerodynamic particle sizer (APS, 0.55 μm-10 μm, aerodynamic diameter). The PSD system sampled from the rooftop with an around 3 m-long sampling tube. A cyclone that removed particles larger than 10 μm was added in front of the sample line.

A Neutral Cluster and Air Ion Spectrometer (NAIS, model 4-11, Airel, Estonia) measures total particle size distribution of 2.5-42 nm (mobility diameter), and ions of 0.7-42 nm, (mobility diameter) (Manninen et al., 2016; Mirme and Mirme, 2013). It switched between detecting either naturally charged ions or total particles (including the uncharged fraction) with unipolar charging. It measured 2 min in the neutral mode, 2 min in the ion mode and then offset for 30 seconds for every measurement cycle. The NAIS was sampling horizontally from the north window. The copper 4 cm outer diameter sampling tube extended 1.6 m outside the window. To increase sampling efficiency the sampling flow rate was 60 lpm.

The trace gas monitors measured carbon monoxide (CO), sulfur dioxide (SO_2), nitrogen oxides (NO_x) and ozone (O_3) concentrations with Thermo Environmental Instruments models 48i, 43i-TLE, 42i, 49i, respectively. They all sampled through a common inlet through the roof of the building. The length of the sampling tube was approximately 3 m.

The $PM_{2.5}$ data was obtained from the nearest national monitor station, Wanliu station, around 3 km north from our station. The $PM_{2.5}$ data from Wanliu station compared nicely to three other adjacent national stations. The data was recorded every hour. Detailed information is reported in (Cao et al., 2014).

2.3 NPF events and haze days classification

We classified days into NPF event days and haze days. The days that did not fit either categories we marked as 'Other day' and they were excluded from our future analysis unless otherwise specified. Table 1 describes the specific calendar of events with the aforementioned categories of days.

We identified the NPF event days following the method introduced in (Dal Maso et al., 2005), which requires an appearance of a new mode below 25 nm and that the new mode shows signs of growth and spans several hours (Dal Maso et al., 2005; Kulmala et al., 2012). Haze days were identified with visibility less than 10 km with ambient relative humidity below 80% (China Meteorological Administration). In this study,

days were classified as haze days when it lasted for at least 12 consecutive hours. In general, there were no overlap between NPF and haze periods. While the NPF events appeared right after sunrise and lasted for several hours, the haze events did not have any specific hour, and lasted for few hours up to several days.

The particle number size distribution was divided into 4 modes according to their diameter: cluster mode (sub-3 nm), nucleation mode (3-25 nm), Aitken mode (25-100 nm), and accumulation mode (100-1000 nm). Moreover, since in Beijing, new particle formation events were only observed during daytime, our analysis concentrated mostly on the time period 8:00 to 14:00, unless specified otherwise.

3 Results and discussion

3.1 General character of particle modes and trace gases

3.1.1 Sub-micron particles and PM2.5

Particle number concentrations of different modes varied depending on the period, as shown in Figure 1. We observed that the cluster and nucleation mode particle concentrations were the highest on NPF event days. In fact, the cluster and nucleation mode particles dominated the total particle number concentration with an average contribution of 96% (Figure 2). On haze days, the average contribution levels of the four modes were equal. Aitken and accumulation mode particles contributed to 52% of the total particle number concentration on the haze days, as compared to 4% on the NPF event days.

On haze days, we observed a surprising concentration of cluster mode particles, which indicates that the clusters in this size range were still produced even during haze. These high concentrations were still present regardless of the high loadings of Aitken and accumulation particles, which are expected to efficiently scavenge the clusters and the smallest growing particles by coagulation (Kerminen et al., 2001; Kulmala et al., 2017). The clusters during haze days could be attributed to a cluster formation which do not grow further (Kulmala et al., 2007), but also to vehicular sources of cluster and nucleation mode particles (e.g. Rönkkö et al., 2017). The ratio between nucleation mode and cluster mode particle median number concentration was close to unity (0.84) which might indicate a concurrent source on haze days, in comparison to the smaller ratio of 0.3 during the NPF days. It is therefore likely that the primary particles dominated the nucleation mode on the haze days, while growth of cluster mode to nucleation mode explains the nucleation mode particles on NPF days.

The median concentrations of Aitken and accumulation mode particles were 17500 cm^{-3} and 17500 cm^{-3}, respectively, during haze days and 8240 cm^{-3} and 1670 cm^{-3}, respectively, during NPF event days. Overall, these concentrations were a factor of 2.1 and 10.5 times higher on the haze days than on the NPF event days. The PM2.5 mass

concentration was clearly higher during haze days than during NPF event days (Figure 3). The $PM_{2.5}$ mass concentration in urban areas is dominated by accumulation mode particles while the contribution of ultrafine (cluster, nucleation and Aitken mode) particles tends to remain relatively little (Feng et al., 2010).

3.1.2 Trace gases

In this work, we considered four trace gases (SO_2, CO, NO_x and O_3) in our analysis (Figure 4), as these compounds are most commonly used to evaluate air quality and pollution sources in China (Hao and Wang, 2005; Han et al., 2011). During our observation period, the median concentrations of SO_2, CO, NO_x on haze days were 5.1, 1400 and 27 ppb, respectively. While still high, these concentrations are lower than the corresponding concentrations (18, 2200, 75 ppb, respectively) during the extremely severe haze episode that took place in Beijing in January 2013 (Wang et al., 2014b).

The median levels of SO_2, CO, NO_x and O_3 were 230%, 50%, 100% and 50% higher, respectively, on haze days than on NPF days. SO_2, CO and NO_x are usually considered tracers of primary pollution, their lower levels on NPF event days than on haze days indicate that new particle formation events favor relatively clean environment (Vahlsing and Smith, 2012;Tian et al., 2018).

3.2 Diurnal behavior

In order to draw a clear picture of the evolution of size-segregated particle number concentrations, we analyzed the diurnal behavior of each of the trace gases (Figure 5) as well as those of particle modes (Figure 6).

Since trace gases have more definitive sources than particles, we can get some insights on particle sources by comparing the diurnal patterns together with particles in different modes. For instance, CO is usually emitted as the by-product of inefficient combustion, biomass burning as well as fossil fuel combustion (Pétron et al., 2004;Lowry et al., 2016). NO_x and CO had similar diurnal patterns. We observed a concurrent increase with morning rush hour followed by another peak at around 15:00. The similar diurnal patterns of CO and NO_x suggest that they have similar sources. Due to lower human activities and traffic during the night, lower concentrations of NO_x and CO were observed. Many observations point out that NO_x and CO are important precursors of O_3 in Chinese urban areas (Wang et al., 2017). Based on our data, O_3, on the other hand, started to increase around 8:00 after the levels of NO_x and CO started to decrease. Ozone had the opposite diurnal pattern to that of NO_x and CO representing the well-known NO_x cycle (Wang et al., 2017).

Interestingly, on haze days, the cluster mode particle number concentration showed a double peak pattern similar to the diurnal cycle of NO_x (Figures 5 & 6). This observation suggests that the clusters on haze days had similar sources as NO_x, plausibly related to combustion. Comparatively, on NPF event days, the cluster mode particle number concentration showed a wide single peak. The cluster mode particle number concentration started to increase at the same time as sunrise, and the peak around noon, showing the typical behavior related to the NPF process (Kulmala et al., 2012).

Similarly, nucleation mode also had a single peak on the NPF event days. Nucleation mode particle number concentration started to increase shortly after the increase of the cluster mode, which could be attributed to the growth of formed particles from the cluster mode into the nucleation mode. The peak however has a shoulder around 7:00 - 9:00 am which is concurrent with the morning peak of NO_x, thus originating from traffic. It is important to note that the height of the peak shoulder of the nucleation mode is only 20% of the maximum nucleation mode number concentration. Our results show that traffic contributes much less to nucleation mode particle number concentration than an NPF event.

During haze days, the diurnal pattern of the nucleation mode overlapped with that of NO_x with no clear major peak during the day. Our observation suggests that the nucleation mode number concentration was dominated by traffic emissions on haze days. Additionally, it is important to note that during haze days, when the main contributor of the nucleation mode particles was traffic, we observed different maximum concentrations for morning versus evening peaks, implying a higher contribution of traffic in the morning than in the afternoon. The result is in line with the diurnal cycle of NO_x during haze days.

Aitken mode particles on NPF days are mainly attributed to two different sources which are hard to distinguish from each other. The Aitken mode particles can be the result of primary or secondary sources, such as combustion and growth of newly formed particles, respectively. In comparison to the cluster and nucleation modes, which had a more pronounced diurnal cycles during the event days, Aitken mode particle number concentration had a similar pattern as NO_x before 9:00 in the morning. This implies that the traffic emissions are important sources to maintain Aitken mode particle concentrations in the morning hours. The Aitken mode concentration increased during the afternoon hours. This is associated with growth of the nucleation mode particles via multicomponent condensation into the Aitken mode sizes. This is verified by a concurrent decrease of nucleation mode particle number concentration. The Aitken mode particle number concentration increase in the afternoon was concurrent with an increase of CO and NO_x, which could be attributed to combustion sources (Roberts and Jones, 2004;Koponen et al., 2001). Similarly, Aitken mode particle concentrations, peak around 20:00 simultaneously with a peak of CO. On haze days, the Aitken mode

particle number concentrations experienced a negligible change before 14:00. Even when CO and NO_x concentration began to decrease, which implies less contribution of primary sources. It is important to mention that growth of particles is not only limited to days when new particle formation occurred. In fact, on haze days, the wind was typically more stagnant reducing vertical mixing of the pollutants and horizontal advection (Zheng et al., 2015). The increase of Aitken mode particle number concentration started around 16:00 and the concentration peaked around 20:00 similar to NPF event days. It is concurrent with the increase time of NO_x and CO, this increase maybe attributed into traffic emission.

The concentration of accumulation mode was an order of magnitude higher during haze days than during NPF days, representing higher condensation sink (0.02 s^{-1} for NPF event days and 0.1 s^{-1} for haze days on average) and thus introducing a reason why NPF does not happen on haze days (Kulmala et al., 2017). The concentration, on the other hand, did not experience much variation during the day. There was a slight increase in during the morning rush hour, starting around 6:00. This is concurrent with the increase in Aitken mode particle number concentration, simultaneous with traffic rush hours in Beijing. The second slight increase started around 16:00, two hours later than that of Aitken mode suggesting the secondary contribution to accumulation mode particles. Accumulation mode also had the similar diurnal pattern as SO_2 on NPF event days, implying SO_2 participated the formation of accumulation mode on the NPF event days.

3.3 Correlation between the particle modes and trace gas concentrations

Beijing's atmosphere is a very complicated environment (Kulmala, 2015). Aerosol particles in the atmosphere of Beijing are subject to e.g. aerosol dynamical processes, surface reactions, coagulation, deposition or transport, thus hindering direct connection with their sources based on physical size distribution only. However, by correlating each particle mode to various trace gases, we can get indications on the sources of the particles. In this section, we use CO, SO_2, NO_x and O_3 as tracers. By evaluating their correlation coefficients with the size segregated particle number concentration (Table 2), we can infer the particle sources. CO, SO_2 and NO_x are primary pollutants emitted from various combustion sources. Our results show that these trace gases have a high positive correlation with accumulation mode particles ($R>0.75$) and negative correlation with cluster and nucleation modes generally.

Figures 7 and 8 show correlation between the size-segregate particle number concentrations and SO_2 and NO_x concentration, respectively.

3.3.1 Connection with SO_2

SO_2 is a key precursor for H_2SO_4 through photochemical reactions in Beijing, which is

in turn a requirement for new particle formation in megacity environments (Wang et al., 2013; Yao et al., 2018). Although a very important precursor of NPF, the SO_2 concentration was lower on NPF event days than on the haze days, relating high concentrations of SO_2 to regional pollution and anthropogenic condensation sink even in semi-pristine environments (Dada et al., 2017). Our observation can be explained by the fact that during haze, SO_2 partitions to the particle and liquid phase oxidation much faster than gas phase oxidation of SO_2 to H_2SO_4. Earlier observations report that the main sources of SO_2 are power plants, traffic and industry, and it can be used as a tracer for regional pollution (Yang et al., 2018;Lu et al., 2010).

Table 2 and Figure 7 show negative correlations between SO_2 concentration and cluster and nucleation mode particle number concentrations, while a highly positive correlation between SO_2 concentration and accumulation mode particle number concentration (R = 0.88), and $PM_{2.5}$ mass concentration (R = 0.80). So, when SO_2 concentration was high, the accumulation mode particle concentration was also high, indicated with high condensation sink yet not limiting aerosol formation.

SO_2 had the highest positive correlation coefficient with the accumulation mode particle number concentration among all the four trace gases. This result suggests that the sources of accumulation mode particles during the time window we chose were more similar to sources of SO_2, attributed to fossil fuel combustion and linked to regional pollution. However, SO_2 contributes to heterogeneous reactions on particle surfaces explaining that a fraction of accumulation mode particles could have resulted from the growth of Aitken mode particles (Ravishankara., 1997).

3.3.2 Connection with NOx

NO_x is usually considered as the pollution tracer mainly from traffic (Beevers et al., 2012). Table 2 and Figure 8 show negative correlation coefficients between NO_x and cluster and nucleation mode particle number concentration and positive correlation coefficients between Aitken and accumulation mode particle number concentration.

As shown in Table 2, the positive correlation coefficient between Aitken mode particle number concentration and NO_x is the highest among all four trace gases. As we mentioned before, traffic is identified as an important source of Aitken and nucleation mode particles. Given that our station is so close to the highway (around 100 m), NO_x concentration is affected by local traffic emissions.

As shown in Figure 8, the higher NO_x concentration was associated with less cluster mode particle number concentration during the NPF event days. However, on haze days the cluster mode particle number concentration seemed not to be sensitive to NO_x concentration, which is in contradiction to our previous understanding that gas phase NO_x can suppress the formation of clusters by suppressing NPF event (Lehtipalo et al.,

2018). However, there might be other sources of cluster mode other than the NPF events as well as compensating vapors that can contribute to clusters formation.

The negative correlation between the NO_x concentration and nucleation mode particle number concentration on the NPF event days can be explained by less cluster mode particles, which act as an important seed for nucleation mode particles. However, on haze days, the negative correlation was slightly higher. On the haze days, primary sources dominated the whole nucleation mode.

The positive correlation between Aitken mode particle number concentration and NO_x concentration on both the NPF event days and the haze days suggests that traffic is one of the major sources of Aitken mode in urban Beijing.

3.4 Correlation between different particle modes

The correlation between size-segregated particle number concentrations (Table 3 and Figure 9) can give us an indication of dynamical behavior of fine particles in the atmosphere aerosols. Generally, pre-existing accumulation mode particles and $PM_{2.5}$ act as coagulation sink and suppress the concentration of cluster mode and nucleation mode particles. The particle number concentrations between adjacent modes were highly correlated except for nucleation mode and Aitken modes. The Aitken mode particles have two different sources e.g. primary emissions and new particle formation events, also they do not necessarily coincide in time. On the other hand, fresh nucleation mode particles must growth fast enough to survive from coagulation scavenging. Only under favorable conditions, nucleation mode particles can grow into Aitken mode particles, resulting increase in Aitken mode number concentration (Kerminen et al., 2001).

Cluster mode particle number concentrations were positively correlated with nucleation mode particle number concentrations on haze days because the traffic emissions were a main primary source of these two modes. On NPF event days, the positive correlation coefficient ($R = 0.84$) between these two modes can be attributed to the growth of clusters into larger particles.

Accumulation mode particle number concentration was positively correlated with Aitken mode particle number concentration on the NPF event days, implying transformation from Aitken mode to accumulation mode. While on haze days, higher Aitken mode particle number concentration was not concurrent with higher accumulation mode particle number concentration. The median Aitken mode particle number concentration was twice on haze days of NPF event days while accumulation mode particle number concentration was 10.5 times on haze days of NPF event days, representing the transformation from Aitken mode to accumulation mode. The high correlation coefficient between accumulation mode particle number concentration and

$PM_{2.5}$ mass concentration implied accumulation mode mainly contributed to $PM_{2.5}$.

4 Conclusion

We investigated the variation of size-segregated particle number concentrations on both NPF and haze days observed during winter 2018 in Beijing. Cluster and nucleation modes contributed to 96% of total sub-micro particle number concentration on NPF days. On haze days, these two modes contributed 48% of the total number concentration while Aitken and accumulation modes contributed to the rest.

Cluster and nucleation modes particle number concentration showed a clear diurnal variation on NPF event days with a typical behavior of NPF events, suggesting NPF event was the main source of these two modes while on the haze days these two modes showed similar diurnal pattern as NO_x, suggesting traffic contributed to these modes.

On NPF event days, the diurnal pattern of Aitken mode particle number concentration showed an increase during traffic rush hour and transformation from nucleation mode. On haze days, the diurnal pattern of Aitken mode particle number concentration still implied secondary sources contribution to this mode. Aitken mode number concentration was highly correlated with NO_x concentration, suggesting traffic emissions contributed to the concentration in this mode.

Accumulation mode particle number concentration showed a similar diurnal pattern as Aitken mode, but no variation on haze days. Accumulation mode was correlated with SO_2, suggesting a character of regional pollution. Accumulation mode mostly contributed to $PM_{2.5}$ mass concentration.

5 Acknowledgments

This study received funding from Beijing University of Chemical Technology. This research has received funding from the National Natural Science Foundation of China (41877306). The work is supported by Academy of Finland via Center of Excellence in Atmospheric Science (project no. 272041) and European Research Council via ATM-GTP 266 (742206). LD received funding from the ATM-DP program at university of Helsinki. KRD acknowledges support by the Swiss National Science postdoc mobility grant P2EZP2_181599. LW acknowledges support by National Key R&D Program of China (2017YFC0209505) and the National Natural Science Foundation of China.

Author contributions. YZ, YiL, YF, JuK contributed to data collection. YZ, TC, LD contributed to data inversion. YZ and LD contributed to analyzing the data. CY, BC, KRD, FB, TK, YoL, JoK contributed to maintaining the station. YZ, LD, JuK, VMK

435 wrote the paper. TP, LW, JJ, MK provided helpful scientific discussions. All co-authors
436 reviewed the manuscript.

437 *Competing interests*. The authors declare that they have no conflict of interest.

438 *Data availability:* Particle number concentrations are available upon contacting
439 yingzhouahl@163.com or lubna.dada@helsinki.fi.

440

6 References

Baklanov, A., Molina, L. T., and Gauss, M.: Megacities, air quality and climate, Atmospheric Environment, 126, 235-249, https://doi.org/10.1016/j.atmosenv.2015.11.059, 2016.

Beevers, S. D., Westmoreland, E., de Jong, M. C., Williams, M. L., and Carslaw, D. C.: Trends in NOx and NO2 emissions from road traffic in Great Britain, Atmospheric Environment, 54, 107-116, https://doi.org/10.1016/j.atmosenv.2012.02.028, 2012.

Cai, R. L., Yang, D. S., Fu, Y. Y., Wang, X., Li, X. X., Ma, Y., Hao, J. M., Zheng, J., and Jiang, J. K.: Aerosol surface area concentration: a governing factor in new particle formation in Beijing, Atmos Chem Phys, 17, 12327-12340, https://doi.org/10.5194/acp-2017-467, 2017.

Cao, C., Jiang, W. J., Wang, B. Y., Fang, J. H., Lang, J. D., Tian, G., Jiang, J. K., and Zhu, T. F.: Inhalable Microorganisms in Beijing's PM2.5 and PM10 Pollutants during a Severe Smog Event, Environ Sci Technol, 48, 1499-1507, https://doi.org/10.1021/es4048472, 2014.

Chu, B. W., Kerminen, V. M., Bianchi, F., Yan, C., Petäjä, T., and Kulmala, M.: Atmospheric new particle formation in China, Atmos Chem Phys, 19, 115-138, https://doi.org/10.5194/acp-19-115-2019, 2019.

Dada, L., Paasonen, P., Nieminen, T., Mazon, S. B., Kontkanen, J., Peräkylä, O., Lehtipalo, K., Hussein, T., Petäjä, T., Kerminen, V. M., Bäck, J., and Kulmala, M.: Long-term analysis of clear-sky new particle formation events and nonevents in Hyytiälä, Atmos Chem Phys, 17, 6227-6241, https://doi.org/10.5194/acp-17-6227-2017, 2017.

Dai, L., Wang, H. L., Zhou, L. Y., An, J. L., Tang, L. L., Lu, C. S., Yan, W. L., Liu, R. Y., Kong, S. F., Chen, M. D., Lee, S. H., and Yu, H.: Regional and local new particle formation events observed in the Yangtze River Delta region, China, J Geophys Res-Atmos, 122, 2389-2402, https://doi.org/10.1002/2016JD026030, 2017.

Dal Maso, M., Kulmala, M., Riipinen, I., Wagner, R., Hussein, T., Aalto, P. P., and Lehtinen, K. E. J.: Formation and growth of fresh atmospheric aerosols: eight years of aerosol size distribution data from SMEAR II, Hyytiala, Finland, Boreal Environ Res, 10, 323-336, 2005.

Feng, X., Dang, Z., Huang, W., Shao, L., and Li, W.: Microscopic morphology and size distribution of particles in PM2.5 of Guangzhou City, Journal of Atmospheric Chemistry, 64, 37-51, http://doi.org/10.1007/s10874-010-9169-7, 2010.

Han, S. Q., Bian, H., Feng, Y. C., Liu, A. X., Li, X. J., Zeng, F., and Zhang, X. L.: Analysis of the Relationship between O3, NO and NO2 in Tianjin, China, Aerosol Air Qual Res, 11, 128-139, https://doi.org/10.4209/aaqr.2010.07.0055, 2011.

Hao, J. M., and Wang, L. T.: Improving urban air quality in China: Beijing case study, J Air Waste Manage, 55, 1298-1305, https://doi.org/10.1080/10473289.2005.10464726, 2005.

Hari, P., and Kulmala, M.: Station for measuring ecosystem-atmosphere relations (SMEAR II), Boreal Environ Res, 10, 315-322, 2005.

IPCC. IPCC, 2007: summary for policymakers. Climate change 2007, 93-129.

Jiang, J. K., Zhao, J., Chen, M. D., Eisele, F. L., Scheckman, J., Williams, B. J., Kuang, C. A., and McMurry, P. H.: First Measurements of Neutral Atmospheric Cluster and 1-2 nm Particle Number Size Distributions During Nucleation Events, Aerosol Science and Technology, 45, Ii-V, https://dio.org/10.1080/02786826.2010.546817, 2011.

Kangasluoma, J., Franchin, A., Duplissy, J., Ahonen, L., Korhonen, F., Attoui, M., Mikkilä, J., Lehtipalo, K., Vanhanen, J., Kulmala, M., and Petäjä, T.: Operation of the Airmodus A11 nano Condensation Nucleus Counter at various inlet pressures and various operation temperatures, and design of a new inlet system, Atmos Meas Tech, 9, 2977-2988, https://doi.org/10.5194/amt-9-2977-2016, 2016.

Kerminen, V. M., Pirjola, L., and Kulmala, M.: How significantly does coagulational scavenging limit atmospheric particle production?, J Geophys Res-Atmos, 106, 24119-24125, https://doi.org/10.1029/2001jd000322, 2001.

Kerminen, V. M., Paramonov, M., Anttila, T., Riipinen, I., Fountoukis, C., Korhonen, H., Asmi, E., Laakso, L., Lihavainen, H., Swietlicki, E., Svenningsson, B., Asmi, A., Pandis, S. N., Kulmala, M., and Petäjä, T.: Cloud condensation nuclei production associated with atmospheric nucleation: a synthesis based on existing literature and new results, Atmos Chem Phys, 12, 12037-12059, https://doi.org/10.5194/acp-12-12037-2012, 2012.

Kerminen, V. M., Chen, X. M., Vakkari, V., Petäjä, T., Kulmala, M., and Bianchi, F.: Atmospheric new particle formation and growth: review of field observations, Environ Res Lett, 13, https://doi.org/10.1088/1748-9326/aadf3c, 2018.

Koponen, I. K., Asmi, A., Keronen, P., Puhto, K., and Kulmala, M.: Indoor air measurement campaign in Helsinki, Finland 1999 - the effect of outdoor air pollution on indoor air, Atmospheric Environment, 35, 1465-1477, https://doi.org/10.1016/s1352-2310(00)00338-1, 2001.

Kreyling, W. G., Semmler, M., and Möller, W.: Dosimetry and toxicology of ultrafine particles, J Aerosol Med, 17, 140-152, https://doi.org/10.1089/0894268041457147, 2004.

Kulmala, M.: How particles nucleate and grow, Science, 302, 1000-1001, https://doi.org/10.1126/science.1090848, 2003.

Kulmala, M., Vehkamäki, H., Petäjä, T., Dal Maso, M., Lauri, A., Kerminen, V. M., Birmili, W., and McMurry, P. H.: Formation and growth rates of ultrafine atmospheric particles: a review of observations, J Aerosol Sci, 35, 143-176, https://doi.org/10.1016/j.jaerosci.2003.10.003, 2004.

Kulmala, M., Riipinen, I., Sipilä, M., Manninen, H. E., Petäjä, T., Junninen, H., Dal Maso, M., Mordas, G., Mirme, A., Vana, M., Hirsikko, A., Laakso, L., Harrison, R. M., Hanson, I., Leung, C., Lehtinen, K. E. J., and Kerminen, V. M.: Toward direct measurement of atmospheric nucleation, Science, 318, 89-92, https://doi.org/10.1126/science.1144124, 2007.

526 Kulmala, M., Petäjä, T., Nieminen, T., Sipilä, M., Manninen, H. E., Lehtipalo, K., Dal
527 Maso, M., Aalto, P. P., Junninen, H., Paasonen, P., Riipinen, I., Lehtinen, K. E. J.,
528 Laaksonen, A., and Kerminen, V. M.: Measurement of the nucleation of
529 atmospheric aerosol particles, Nat Protoc, 7, 1651-1667,
530 https://doi.org/10.1038/nprot.2012.091, 2012.
531 Kulmala, M., Kontkanen, J., Junninen, H., Lehtipalo, K., Manninen, H. E., Nieminen,
532 T., Petäjä, T., Sipilä, M., Schobesberger, S., Rantala, P., Franchin, A., Jokinen, T.,
533 Järvinen, E., Äijälä, M., Kangasluoma, J., Hakala, J., Aalto, P. P., Paasonen, P.,
534 Mikkilä, J., Vanhanen, J., Aalto, J., Hakola, H., Makkonen, U., Ruuskanen, T.,
535 Mauldin, R. L., Duplissy, J., Vehkamäki, H., Bäck, J., Kortelainen, A., Riipinen,
536 I., Kurtén, T., Johnston, M. V., Smith, J. N., Ehn, M., Mentel, T. F., Lehtinen, K.
537 E. J., Laaksonen, A., Kerminen, V. M., and Worsnop, D. R.: Direct Observations
538 of Atmospheric Aerosol Nucleation, Science, 339, 943-946,
539 https://doi.org/10.1126/science.1227385, 2013.
540 Kulmala, M.: Atmospheric chemistry: China's choking cocktail, Nature, 526, 497-499,
541 https://doi.org/10.1038/526497a, 2015.
542 Kulmala, M., Kerminen, V. M., Petäjä, T., Ding, A. J., and Wang, L.: Atmospheric gas-
543 to-particle conversion: why NPF events are observed in megacities?, Faraday
544 Discuss, 200, 271-288, https://doi.org/10.1039/C6FD00257A, 2017.
545 Lehtipalo, K., Yan, C., Dada, L., Bianchi, F., Xiao, M., Wagner, R., Stolzenburg, D.,
546 Ahonen, L. R., Amorim, A., Baccarini, A., Bauer, P. S., Baumgartner, B., Bergen,
547 A., Bernhammer, A. K., Breitenlechner, M., Brilke, S., Buchholz, A., Mazon, S.
548 B., Chen, D. X., Chen, X. M., Dias, A., Dommen, J., Draper, D. C., Duplissy, J.,
549 Ehn, M., Finkenzeller, H., Fischer, L., Frege, C., Fuchs, C., Garmash, O., Gordon,
550 H., Hakala, J., He, X. C., Heikkinen, L., Heinritzi, M., Helm, J. C., Hofbauer, V.,
551 Hoyle, C. R., Jokinen, T., Kangasluoma, J., Kerminen, V. M., Kim, C., Kirkby, J.,
552 Kontkanen, J., Kurten, A., Lawler, M. J., Mai, H. J., Mathot, S., Mauldin, R. L.,
553 Molteni, U., Nichman, L., Nie, W., Nieminen, T., Ojdanic, A., Onnela, A.,
554 Passananti, M., Petäjä, T., Piel, F., Pospisilova, V., Quéléver, L. L. J., Rissanen,
555 M. P., Rose, C., Sarnela, N., Schallhart, S., Schuchmann, S., Sengupta, K., Simon,
556 M., Sipilä, M., Tauber, C., Tomé, A., Tröstl, J., Väisänen, O., Vogel, A. L.,
557 Volkamer, R., Wagner, A. C., Wang, M. Y., Weitz, L., Wimmer, D., Ye, P. L.,
558 Ylisirnio, A., Zha, Q. Z., Carslaw, K. S., Curtius, J., Donahue, N. M., Flagan, R.
559 C., Hansel, A., Riipinen, I., Virtanen, A., Winkler, P. M., Baltensperger, U.,
560 Kulmala, M., and Worsnop, D. R.: Multicomponent new particle formation from
561 sulfuric acid, ammonia, and biogenic vapors, Sci Adv, 4,
562 https://doi.org/10.1126/sciadv.aau5363, 2018.
563 Lelieveld, J., Evans, J. S., Fnais, M., Giannadaki, D., and Pozzer, A.: The contribution
564 of outdoor air pollution sources to premature mortality on a global scale, Nature,
565 525, 367-371, https://doi.org/10.1038/nature15371,2015.
566 Liu, J. Q., Jiang, J. K., Zhang, Q., Deng, J. G., and Hao, J. M.: A spectrometer for
567 measuring particle size distributions in the range of 3 nm to 10 mu m, Front Env
568 Sci Eng, 10, 63-72, https://doi.org/10.1007/s11783-014-0754-x,2016.

569 Lowry, D., Lanoiselle, M. E., Fisher, R. E., Martin, M., Fowler, C. M. R., France, J. L.,
570 Hernandez-Paniagua, I. Y., Novelli, P. C., Sriskantharajah, S., O'Brien, P., Rata,
571 N. D., Holmes, C. W., Fleming, Z. L., Clemitshaw, K. C., Zazzeri, G., Pommier,
572 M., McLinden, C. A., and Nisbet, E. G.: Marked long-term decline in ambient
573 CO mixing ratio in SE England, 1997-2014: evidence of policy success in
574 improving air quality, Sci Rep-Uk, 6, https://doi.org/10.1038/srep25661, 2016.
575 Lu, Y., Yan, C., Fu, Y., Chen, Y., Liu, Y., Yang, G., Wang, Y., Bianchi, F., Chu, B., Zhou,
576 Y., Yin, R., Baalbaki, R., Garmash, O., Deng, C., Wang, W., Liu, Y., Petäjä, T.,
577 Kerminen, V. M., Jiang, J., Kulmala, M., and Wang, L.: A proxy for atmospheric
578 daytime gaseous sulfuric acid concentration in urban Beijing, Atmos. Chem. Phys.
579 Discuss., 2018, 1-31, https://doi.org/10.5194/acp-2018-1132, 2018.
580 Lu, Z., Streets, D. G., Zhang, Q., Wang, S., Carmichael, G. R., Cheng, Y. F., Wei, C.,
581 Chin, M., Diehl, T., and Tan, Q.: Sulfur dioxide emissions in China and sulfur
582 trends in East Asia since 2000, Atmos Chem Phys, 10, 6311-6331,
583 https://doi.org/10.5194/acp-10-6311-2010, 2010.
584 Manninen, H. E., Mirme, S., Mirme, A., Petäjä, T., and Kulmala, M.: How to reliably
585 detect molecular clusters and nucleation mode particles with Neutral cluster and
586 Air Ion Spectrometer (NAIS), Atmos Meas Tech, 9, 3577-3605,
587 https://doi.org/10.5194/amt-9-3577-2016, 2016.
588 Mirme, A., Tamm, E., Mordas, G., Vana, M., Uin, J., Mirme, S., Bernotas, T., Laakso,
589 L., Hirsikko, A., and Kulmala, M.: A wide-range multi-channel air ion
590 spectrometer, Boreal Environ Res, 12, 247-264, 2007.
591 Mirme, S., and Mirme, A.: The mathematical principles and design of the NAIS - a
592 spectrometer for the measurement of cluster ion and nanometer aerosol size
593 distributions, Atmos Meas Tech, 6, 1061-1071, https://doi.org/10.5194/amt-6-
594 1061-2013, 2013.
595 Oberdörster, G., Sharp, Z., Atudorei, V., Elder, A., Gelein, R., Kreyling, W., and Cox,
596 C.: Translocation of inhaled ultrafine particles to the brain, Inhal Toxicol, 16, 437-
597 445, https://doi.org/10.1080/08958370490439597, 2004.
598 Pétron, G., Granier, C., Khattatov, B., Yudin, V., Lamarque, J. F., Emmons, L., Gille, J.,
599 and Edwards, D. P.: Monthly CO surface sources inventory based on the 2000-
600 2001 MOPITT satellite data, Geophys Res Lett, 31,
601 https://doi.org/10.1029/2004gl020560, 2004.
602 Pirjola, L., Lähde, T., Niemi, J. V., Kousa, A., Rönkkö, T., Karjalainen, P., Keskinen, J.,
603 Frey, A., and Hillamo, R.: Spatial and temporal characterization of traffic
604 emissions in urban microenvironments with a mobile laboratory, Atmospheric
605 Environment, 63, 156-167, https://doi.org/10.1016/j.atmosenv.2012.09.022,
606 2012.
607 Ravishankara, A.R.: Heterogeneous and Multiphase Chemistry in the Troposphere,
608 Science 276, 1058-1065, https://doi.org/ 10.1126/science.276.5315.1058,1997.
609 Roberts, D. L., and Jones, A.: Climate sensitivity to black carbon aerosol from fossil
610 fuel combustion, J Geophys Res-Atmos, 109,
611 https://doi.org/10.1029/2004jd004676, 2004.

612 Rönkkö, T., Kuuluvainen, H., Karjalainen, P., Keskinen, J., Hillamo, R., Niemi, J. V.,
613 Pirjola, L., Timonen, H. J., Saarikoski, S., Saukko, E., Järvinen, A., Silvennoinen,
614 H., Rostedt, A., Olin, M., Yli-Ojanperä, J., Nousiainene, P., Kousa, A., and Dal
615 Maso, M.: Traffic is a major source of atmospheric nanocluster aerosol, P Natl
616 Acad Sci USA, 114, 7549-7554, https://doi.org/10.1073/pnas.1700830114, 2017.
617 Solomos, S., Kallos, G., Kushta, J., Astitha, M., Tremback, C., Nenes, A., and Levin,
618 Z.: An integrated modeling study on the effects of mineral dust and sea salt
619 particles on clouds and precipitation, Atmos Chem Phys, 11, 873-892,
620 https://doi.org/10.5194/acp-11-873-2011, 2011.
621 Tian, X., Xie, P. H., Xu, J., Li, A., Wang, Y., Qin, M., and Hu, Z. K.: Long-term
622 observations of tropospheric NO2, SO2 and HCHO by MAX-DOAS in Yangtze
623 River Delta area, China, J Environ Sci-China, 71, 207-221,
624 https://doi.org/10.1016/j.jes.2018.03.006, 2018.
625 Vahlsing, C., and Smith, K. R.: Global review of national ambient air quality standards
626 for PM10 and SO2 (24 h), Air Qual Atmos Hlth, 5, 393-399,
627 https://doi.org/10.1007/s11869-010-0131-2, 2012.
628 Vanhanen, J., Mikkilä, J., Lehtipalo, K., Sipilä, M., Manninen, H. E., Siivola, E., Petäjä,
629 T., and Kulmala, M.: Particle Size Magnifier for Nano-CN Detection, Aerosol
630 Science and Technology, 45, 533-542,
631 https://doi.org/10.1080/02786826.2010.547889, 2011.
632 von Bismarck-Osten, C., Birmili, W., Ketzel, M., Massling, A., Petäjä, T., and Weber,
633 S.: Characterization of parameters influencing the spatio-temporal variability of
634 urban particle number size distributions in four European cities, Atmospheric
635 Environment, 77, 415-429, https://doi.org/10.1016/j.atmosenv.2013.05.029,
636 2013.
637 Wang, D. W., Guo, H., Cheung, K., and Gan, F. X.: Observation of nucleation mode
638 particle burst and new particle formation events at an urban site in Hong Kong,
639 Atmospheric Environment, 99, 196-205,
640 https://doi.org/10.1016/j.atmosenv.2014.09.074, 2014a.
641 Wang, T., Xue, L. K., Brimblecombe, P., Lam, Y. F., Li, L., and Zhang, L.: Ozone
642 pollution in China: A review of concentrations, meteorological influences,
643 chemical precursors, and effects, Science of the Total Environment, 575, 1582-
644 1596, https://doi.org/10.1016/j.scitotenv.2016.10.081, 2017.
645 Wang, Y. S., Yao, L., Wang, L. L., Liu, Z. R., Ji, D. S., Tang, G. Q., Zhang, J. K., Sun,
646 Y., Hu, B., and Xin, J. Y.: Mechanism for the formation of the January 2013 heavy
647 haze pollution episode over central and eastern China, Sci China Earth Sci, 57,
648 14-25, https://doi.org/10.1007/s11430-013-4773-4, 2014b.
649 Wang, Z. B., Hu, M., Wu, Z. J., Yue, D. L., He, L. Y., Huang, X. F., Liu, X. G., and
650 Wiedensohler, A.: Long-term measurements of particle number size distributions
651 and the relationships with air mass history and source apportionment in the
652 summer of Beijing, Atmos Chem Phys, 13, 10159-10170,
653 https://doi.org/10.5194/acp-13-10159-2013, 2013.
654 Wehner, B., Wiedensohler, A., Tuch, T. M., Wu, Z. J., Hu, M., Slanina, J., and Kiang,
655 C. S.: Variability of the aerosol number size distribution in Beijing, China: New

656 particle formation, dust storms, and high continental background, Geophys Res
657 Lett, 31, https://doi.org/10.1029/2004GL021596, 2004.
658 WHO. Health and health behaviour among young people: health behaviour in school-
659 aged children: a WHO cross-national study (HBSC), international report; WHO:
660 2000.
661 Wu, Z. J., Hu, M., Lin, P., Liu, S., Wehner, B., and Wiedensohler, A.: Particle number
662 size distribution in the urban atmosphere of Beijing, China, Atmospheric
663 Environment, 42, 7967-7980, https://doi.org/10.1016/j.atmosenv.2008.06.022,
664 2008.
665 Xiao, S., Wang, M. Y., Yao, L., Kulmala, M., Zhou, B., Yang, X., Chen, J. M., Wang,
666 D. F., Fu, Q. Y., Worsnop, D. R., and Wang, L.: Strong atmospheric new particle
667 formation in winter in urban Shanghai, China, Atmos Chem Phys, 15, 1769-1781,
668 https://doi.org/10.5194/acp-15-1769-2015, 2015.
669 Yang, M., Ma, T. M., and Sun, C. W.: Evaluating the impact of urban traffic investment
670 on SO2 emissions in China cities, Energ Policy, 113, 20-27,
671 https://doi.org/10.1016/j.enpol.2017.10.039, 2018.
672 Yao, L., Garmash, O., Bianchi, F., Zheng, J., Yan, C., Kontkanen, J., Junninen, H.,
673 Mazon, S. B., Ehn, M., Paasonen, P., Sipilä, M., Wang, M. Y., Wang, X. K., Xiao,
674 S., Chen, H. F., Lu, Y. Q., Zhang, B. W., Wang, D. F., Fu, Q. Y., Geng, F. H., Li,
675 L., Wang, H. L., Qiao, L. P., Yang, X., Chen, J. M., Kerminen, V. M., Petäjä, T.,
676 Worsnop, D. R., Kulmala, M., and Wang, L.: Atmospheric new particle formation
677 from sulfuric acid and amines in a Chinese megacity, Science, 361, 278-281,
678 https://doi.org/10.1126/science.aao4839, 2018.
679 Yu, H., Zhou, L. Y., Dai, L., Shen, W. C., Dai, W., Zheng, J., Ma, Y., and Chen, M. D.:
680 Nucleation and growth of sub-3nm particles in the polluted urban atmosphere of
681 a megacity in China, Atmos Chem Phys, 16, 2641-2657,
682 http://doi.org/10.5194/acp-16-2641-2016, 2016.
683 Yue, D. L., Hu, M., Wu, Z. J., Guo, S., Wen, M. T., Nowak, A., Wehner, B.,
684 Wiedensohler, A., Takegawa, N., Kondo, Y., Wang, X. S., Li, Y. P., Zeng, L. M.,
685 and Zhang, Y. H.: Variation of particle number size distributions and chemical
686 compositions at the urban and downwind regional sites in the Pearl River Delta
687 during summertime pollution episodes, Atmos Chem Phys, 10, 9431-9439,
688 https://doi.org/10.5194/acp-10-9431-2010, 2010.
689 Zheng, G. J., Duan, F. K., Su, H., Ma, Y. L., Cheng, Y., Zheng, B., Zhang, Q., Huang,
690 T., Kimoto, T., Chang, D., Pöschl, U., Cheng, Y. F., and He, K. B.: Exploring the
691 severe winter haze in Beijing: the impact of synoptic weather, regional transport
692 and heterogeneous reactions, Atmos Chem Phys, 15, 2969-2983,
693 https://doi.org/10.5194/acp-15-2969-2015, 2015.
694
695
696
697

Atmos. Chem. Phys. Discuss., https://doi.org/10.5194/acp-2019-60
Manuscript under review for journal Atmos. Chem. Phys.
Discussion started: 13 March 2019

698 Tables and Figures

699 Table 1. Calendar of events during our observation. NPF event days are marked in green,
700 haze days are marked in grey. Missing or undefined days are marked in white.

701

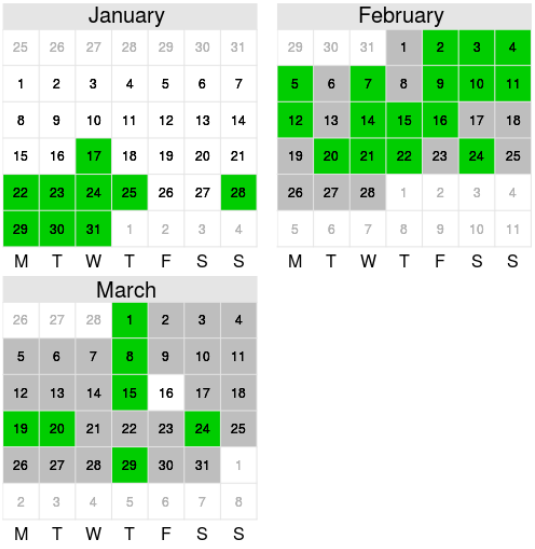

702

Atmos. Chem. Phys. Discuss., https://doi.org/10.5194/acp-2019-60
Manuscript under review for journal Atmos. Chem. Phys.
Discussion started: 13 March 2019

Atmospheric Chemistry and Physics Discussions

703

704 Table 2. Correlation coefficients between size segregated number concentrations /
705 $PM_{2.5}$ and trace gases mixing ratios. The time window is 08:00 - 14:00. All the data are
706 in log scale, high correlation coefficients (|R|>0.7) have been marked in blue and the
707 extremely high correlation coefficient (|R|>0.8) is marked in red. The R between trace
708 gases / $PM_{2.5}$ and Cluster mode include 1770 data points (12 minutes averaged value)
709 for each parameter, R between trace gases / $PM_{2.5}$ and Nucleation, Aitken and
710 Accumulation mode includes 4248 data points (5 minutes averaged value) for each
711 parameter.

R	CO	SO_2	NO_x	O_3
Cluster	-0.71	-0.65	**-0.71**	0.06
Nucleation	-0.60	-0.60	-0.68	0.07
Aitken	0.61	0.61	**0.79**	-0.28
Accumulation	**0.79**	**0.88**	**0.78**	0.16
$PM_{2.5}$	**0.77**	**0.80**	0.70	0.36

712

713

Atmos. Chem. Phys. Discuss., https://doi.org/10.5194/acp-2019-60
Manuscript under review for journal Atmos. Chem. Phys.
Discussion started: 13 March 2019

Atmospheric Chemistry and Physics Discussions

Table 3: Correlation coefficient between size-segregated particle number concentrations / $PM_{2.5}$. The time window is 08:00 - 14:00. All the data are in log scale, high correlation coefficients (|R|>0.8) have been marked in blue. And the extremely high correlation coefficients are marked in red (|R|>0.9). The R between Cluster and other modes / $PM_{2.5}$ include 1770 data points (12 minutes averaged value) for each parameter. R between any modes else than Cluster mode include 4248 data points (5 minutes averaged value) for each parameter.

R	Cluster	Nucleation	Aitken	Accumulation	$PM_{2.5}$
Cluster	1				
Nucleation	**0.84**	1			
Aitken	-0.53	-0.47	1		
Accumulation	**-0.84**	-0.72	0.66	1	
$PM_{2.5}$	**-0.84**	-0.71	0.47	**0.92**	1

Atmos. Chem. Phys. Discuss., https://doi.org/10.5194/acp-2019-60
Manuscript under review for journal Atmos. Chem. Phys.
Discussion started: 13 March 2019

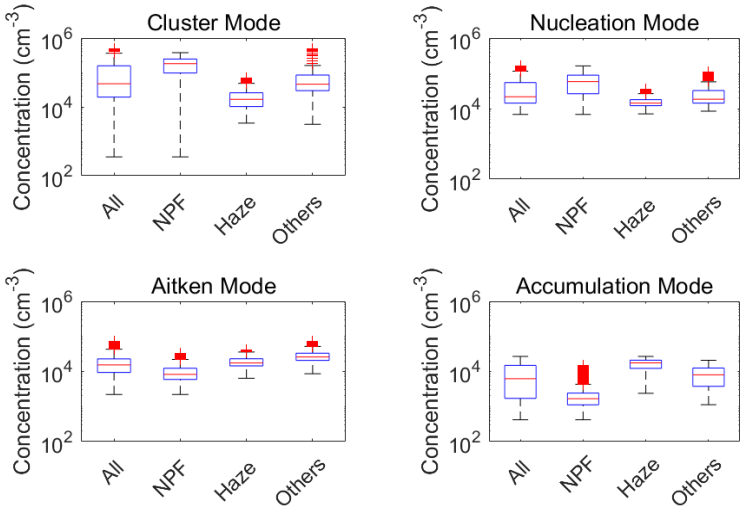

723

724 Figure 1. Particle number concentrations in the cluster, nucleation, Aitken and
725 accumulation mode on all days, NPF event days, haze days and other days. The
726 whiskers include 99.3% of data of every group. Data out of 1.5 x interquartile range are
727 posited outside the whiskers and considered as outliers. This figure shows median and
728 percentiles of size-segregated particle number concentration. The lines in the boxes
729 represent the median value, the lower of the boxes represent 25% of the mixing ratio
730 and the upper of the boxes represent 75% of the mixing ratio. Data marked with red
731 pluses represent outliers.

732

Atmos. Chem. Phys. Discuss., https://doi.org/10.5194/acp-2019-60
Manuscript under review for journal Atmos. Chem. Phys.
Discussion started: 13 March 2019

Atmospheric Chemistry and Physics Discussions

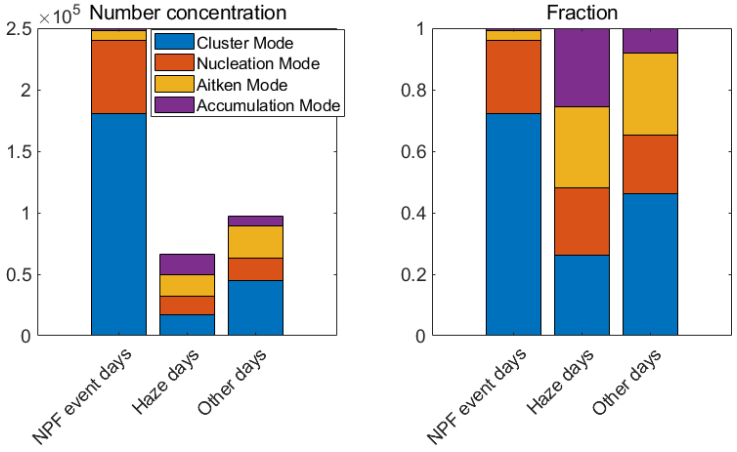

733

734 Figure 2. Fractions of each mode under different conditions. The plot on the right is
735 median size-segregated number concentrations on NPF event days, haze days and other
736 days. The plot on the left is the fraction of median number concentration of each mode.

737

Atmos. Chem. Phys. Discuss., https://doi.org/10.5194/acp-2019-60
Manuscript under review for journal Atmos. Chem. Phys.
Discussion started: 13 March 2019

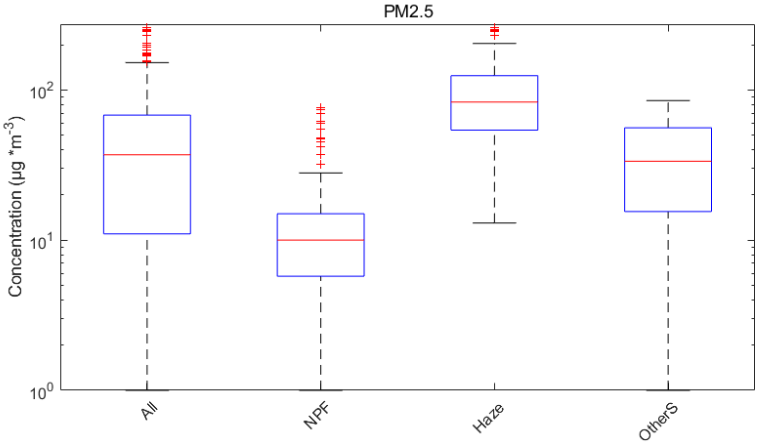

738

739 Figure 3. General character of $PM_{2.5}$ mass concentration on all days, NPF event days,
740 haze days, and others days separately. This figure shows median and percentiles of
741 $PM_{2.5}$ mass concentration. The lines in the boxes represent the median value, the lower
742 of the boxes represent 25% of the data and the upper of the boxes represent 75% of the
743 data. Data marked with red pluses represent outliers as in Figure 1.

744

Atmos. Chem. Phys. Discuss., https://doi.org/10.5194/acp-2019-60
Manuscript under review for journal Atmos. Chem. Phys.
Discussion started: 13 March 2019

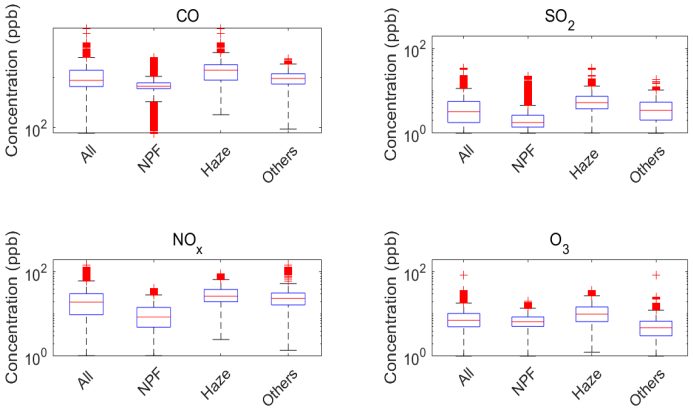

Figure 4. Trace gases mixing ratios of CO, SO_2, NO_x and O_3 on all days, NPF event days, haze days and other days. This figure shows median and percentiles of trace gases. The lines in the boxes represent the median value, the lower of the boxes represent 25% of the data and the upper of the boxes represent 75% of the data. Data marked with red pluses represent outliers as in Figure 1.

Atmos. Chem. Phys. Discuss., https://doi.org/10.5194/acp-2019-60
Manuscript under review for journal Atmos. Chem. Phys.
Discussion started: 13 March 2019

753

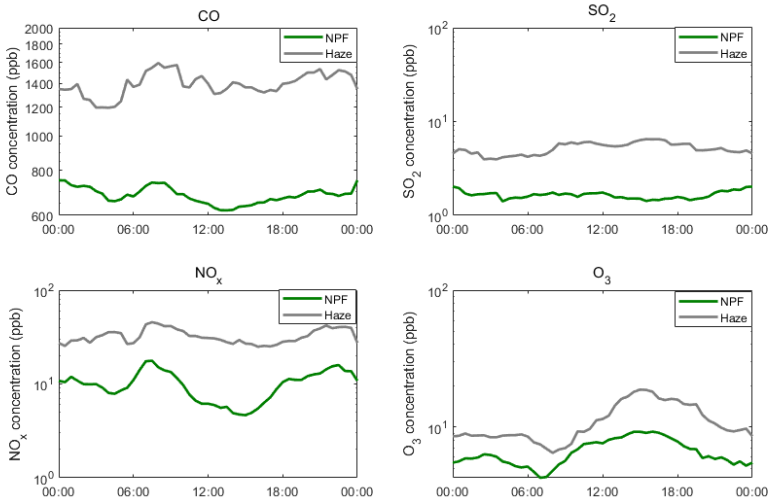

754

755 Figure 5. Diurnal variation of trace gases (CO, SO_2, NO_x and O_3 separately) mixing
756 ratio on haze days (grey lines) and NPF event days (green lines), and they are the
757 median data from midnight to midnight.

758

Atmos. Chem. Phys. Discuss., https://doi.org/10.5194/acp-2019-60
Manuscript under review for journal Atmos. Chem. Phys.
Discussion started: 13 March 2019

Atmospheric Chemistry and Physics Discussions

759

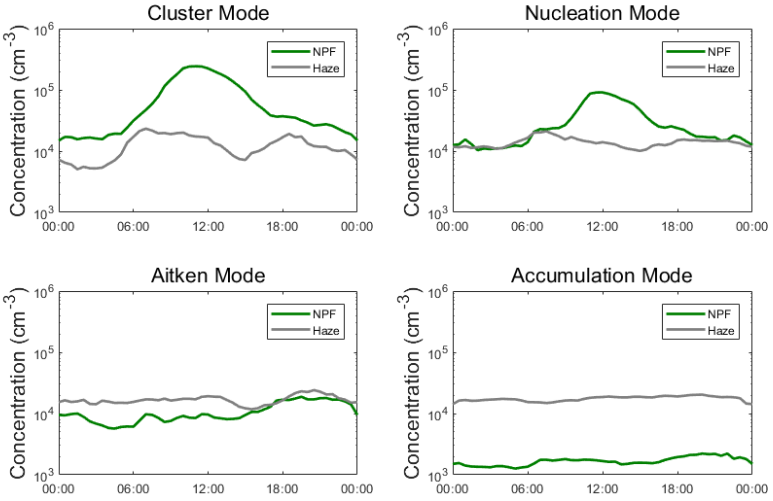

760

761 Figure 6. Diurnal variation of particles (cluster, nucleation, Aitken and accumulation
762 mode separately) number concentration on haze days (grey lines) and NPF event days
763 (green lines), and they are the median data from midnight to midnight.

764

Atmos. Chem. Phys. Discuss., https://doi.org/10.5194/acp-2019-60
Manuscript under review for journal Atmos. Chem. Phys.
Discussion started: 13 March 2019

765

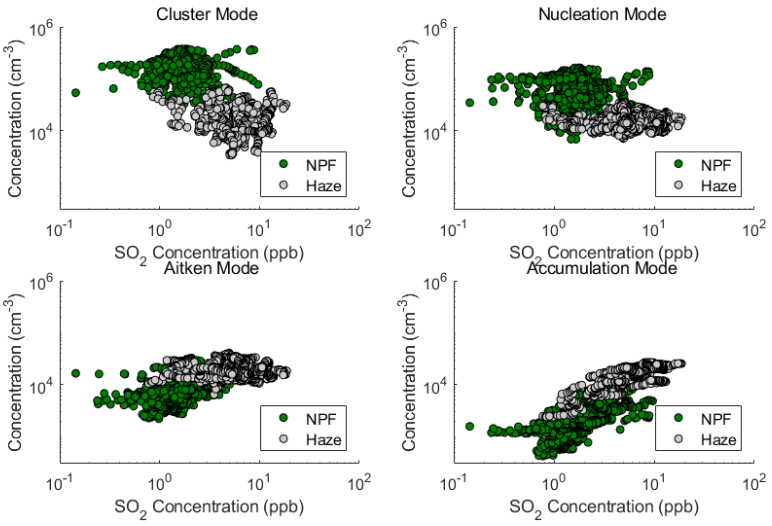

766

767 Figure 7. Relation between the SO_2 concentration and particle number concentration in
768 each mode. The time resolution of the data points are 1 hour.

769

Atmos. Chem. Phys. Discuss., https://doi.org/10.5194/acp-2019-60
Manuscript under review for journal Atmos. Chem. Phys.
Discussion started: 13 March 2019

Atmospheric Chemistry and Physics Discussions

770

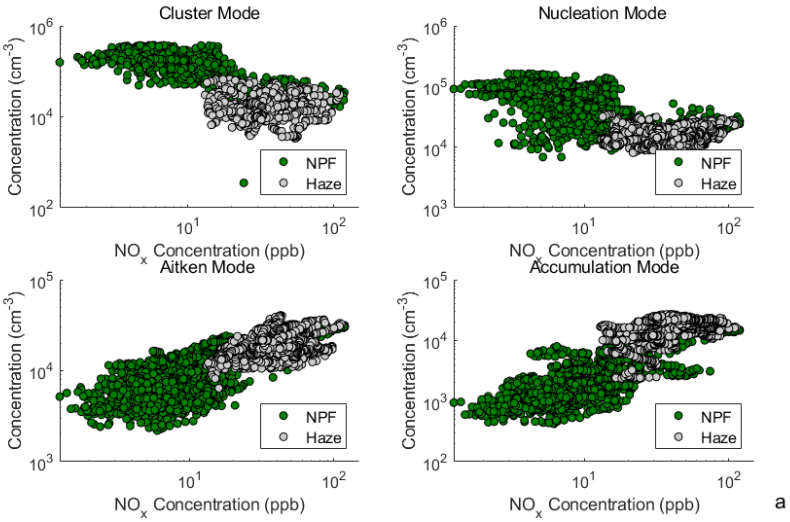

771

772 Figure 8. Relation between the NOx concentration and particle number concentration
773 in each mode. The time resolution of the data points are 1 hour.

774

Atmos. Chem. Phys. Discuss., https://doi.org/10.5194/acp-2019-60
Manuscript under review for journal Atmos. Chem. Phys.
Discussion started: 13 March 2019

Atmospheric Chemistry and Physics Discussions

775

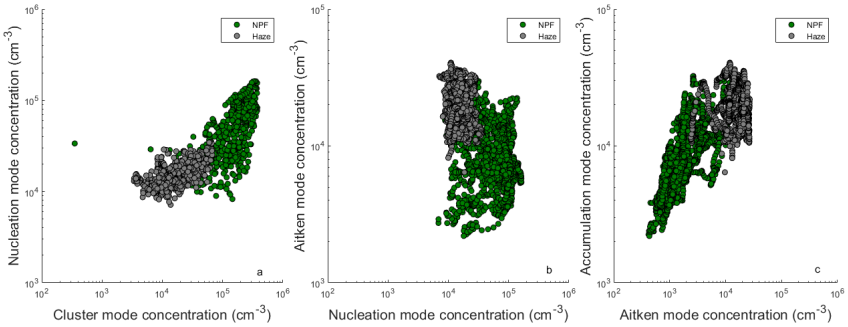

776

777

778 Figure 9. Correlations between particle number concentration in neighboring modes.
779 The time resolution of the data points are 1 hour.